

TOMOGRAPHY AS A DIAGNOSTIC TOOL FOR PLASMA ETCHING OF SRF CAVITIES

M. Nikolić, F. Čučkov, A. Samolov, A. Godunov, S. Popović, and L. Vušković
Center for Accelerator Science, Old Dominion University, Norfolk VA

Abstract

Plasma based surface modification is a promising alternative for etching of superconductive radio frequency (SRF) cavities. A plasma processed SRF cavity presents a plasma reactor with a limited or distorted symmetry. We are developing a tomographic reconstruction of local plasma parameters, as a diagnostic tool in the plasma etching setting of SRF cavities. The method is non-invasive and provides deep insight into the fundamental processes and phenomena during the plasma treatment of the surfaces of SRF cavities. Here we report on our progress in developing a tomographic numerical method, based on the 2D inverse Radon formula. We tested it on supersonic flowing microwave discharge maintained in a cylindrical quartz tube. Due to the models sensitivity to the noise signal in the experiment, an automated measurement system has been built with the aim to increase the overall precision of data acquisition, as well as to streamline the measurement process.

INTRODUCTION

Recently, there has been an increasing interest for dry, plasma based, etching technologies of SRF niobium cavities. These technologies are low cost, environmentally friendly, easy controllable and present a possible alternative to currently used acid based wet technologies, such as buffered chemical polishing (BCP), or electrochemical polishing (EP). A similar approach has already been employed in preparation of superconducting devices and it is a vital technology in semiconductor material processing. Experiments done on flat samples showed that the surface roughness of plasma etched samples is comparable to the chemically etched samples [1].

The geometry of SRF cavities requires the RF discharge to be asymmetric. To investigate these asymmetric discharges and their properties, we employed a tomographic analysis based on the 2D inverse Radon formula. Two dimensional tomography explores the internal dynamics of the observed discharge. Since plasma is a highly radiating object, emission tomography was engaged to avoid perturbing the system while taking measurements. We used several computer tomography methods for the characterization of this plasma object to study its collective behavior.

EXPERIMENTAL APPROACH

We tested the applicability of the tomography model on the argon microwave discharge maintained in the cylindrical quartz cavity at atmospheric pressures, Fig. 1. A commercial microwave generator, operating in the S-band

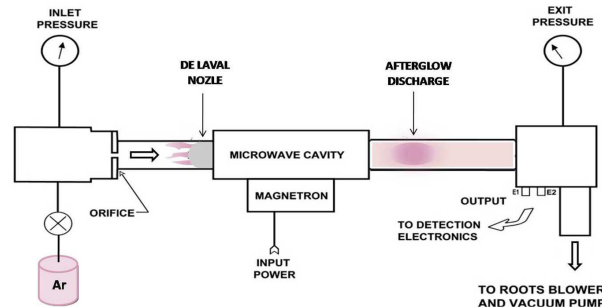


Figure 1: Scheme of the supersonic flowing microwave discharge.

at 2.45 GHz, was used to sustain a cylindrical cavity discharge at power density of 4 W/cm^3 . Supersonic flow was generated with a Mach 2 cylindrical convergent-divergent De Laval nozzle by using an evacuated quartz tube as a wave guide.

Optical emission spectroscopy was used for a detailed characterization of the afterglow region of the supersonic flowing discharge. The spectroscopy measurements were taken at different positions and under different angles to observe populations of excited species in the afterglow region. All spectral measurements were performed side-on with respect to the direction of the discharge flow.

We used a Newport/Oriel absolute black body irradiance source to calibrate the observed spectra and obtain graphs of spectral irradiance per count versus wavelength. The population of particular excited state transitions were determined by using these graphs.

An automated measurement system (AMS) has been built in order to increase both the angle and the distance measurement precision. A photo of the AMS is shown in Fig. 2. It consists of a mirror and a microcontroller-based system, composed of two high-precision stepper motors and several sensors providing precise feedback control. This allowed us to resolve the angle and distance on a sub-degree and sub-milimeter scale, respectively. The mirror reflectivity was determined independently and then included in the data calibration. Measurements were taken under 21 angles in the range from 48 to 168 degrees and 17 projections for each angle in 0.2 cm increments across the quartz tube cross section.

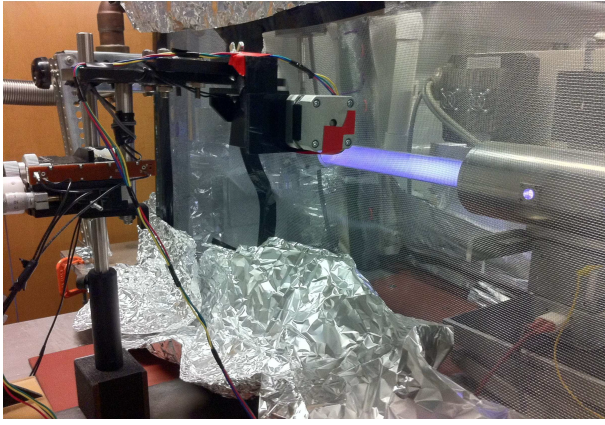


Figure 2: A photo of an automated measurement system.

PLASMA TOMOGRAPHY

Radon Transform

Spectral line intensities of observed atomic emitters show only the integrated effects of collective plasma behaviour. If we want to look into the internal dynamics of the discharge, it is necessary to transform these integrated data into the spatial population distributions, $\epsilon(x, y)$, Fig. 3. Radon transform provides the information about measured line intensities dependence on $\epsilon(x, y)$.

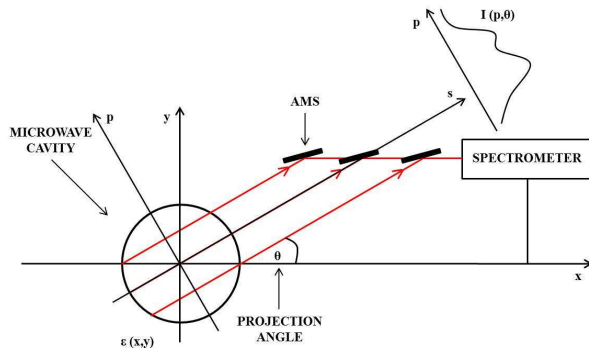


Figure 3: Scheme of experimental set-up for the plasma tomography experiment.

Measured spectral line intensities are connected to the spatial population distributions with the Radon formula [2],

$$I(p, \theta) = \int_L \epsilon(x, y) ds, \quad (1)$$

where

$$s = x \cos \theta + y \sin \theta \quad (2)$$

$$p = -x \sin \theta + y \cos \theta \quad (3)$$

where L is the line of integration and ds is the increment of the length along that line.

By applying the inverse Radon transformation in the spatial domain and using the Fourier slice theorem [3], we ob-

tained the spatial population distributions,

$$\epsilon(x, y) = \int_0^\pi d\theta \int_{-\infty}^{\infty} F^{-1}(|\nu|) I(p, \theta) dp. \quad (4)$$

Knowing the inverse Fourier transform of the function $|\nu|$ [5]

$$F^{-1}(|\nu|) = -\frac{1}{2\pi^2 p^2}, \quad (5)$$

we obtain

$$\epsilon(x, y) = -\frac{1}{2\pi^2} \int_0^\pi d\theta \int_{-\infty}^{\infty} \frac{I(p, \theta)}{(p - p_0)^2} dp, \quad (6)$$

where

$$p_0 = -x \sin \theta + y \cos \theta. \quad (7)$$

It is obvious from Eq. (6) that the inverse Radon integral has a singular point at $p = p_0$ and will be difficult to solve. Also, the Radon formula is rigorously valid for continuous functions with compact support, or for infinite set of projections. The singularity can be avoided mathematically if the integral in Eq. (6) corresponds to the Cauchy principal value integral [4], but even then some information may be lost in the reconstruction process due to lack of noise filtering. A possible solution is to apply the filtered-back projection (FBP) algorithm.

Filtered-back Projection

We start by calculating a filtered projection $Q_\theta(p)$ for each projection $I_\theta(p)$ [5]. Then, Eq. (4) can be rewritten as

$$\epsilon(x, y) = \int_0^\pi Q_\theta(-x \sin \theta + y \cos \theta) d\theta. \quad (8)$$

If we cut off higher frequencies in the spatial domain, the filtered projection is of the form

$$Q_\theta(p) = \int_{-\infty}^{\infty} I_\theta(p') h(p - p') dp', \quad (9)$$

where $h(p)$ is a filter which purpose is to cut off higher frequencies, since higher frequency signals are attributed to noise.

Experimentally obtained line intensities are usually presented as a discrete set of projections, measured with the spatial sampling interval τ , thus $p = n\tau$, where n is an integer. If we assume that each projection $I_\theta(k\tau)$ is zero outside the index range $k = 0, 1, \dots, K - 1$, we may express the *filtered projection* as

$$Q_\theta(n\tau) = \tau \sum_{k=0}^{K-1} h(n\tau - k\tau) I_\theta(k\tau) \quad (10)$$

$$n = 0, 1, \dots, K - 1.$$

Finally the reconstructed function $\epsilon(x, y)$ may be obtained by the discrete approximation of the Eq. (8)

$$\epsilon(x, y) = \frac{\pi}{K} \sum_{i=1}^K Q_{\theta_i}(-x \sin \theta_i + y \cos \theta_i), \quad (11)$$

where the K angles are the ones at which the projections are sampled. This means that each filtered projection has to be back-projected.

The most commonly used filters are the *Ram-Lak* filter [6]

$$h(n\tau) = \begin{cases} \frac{1}{4\tau^2}, & n = 0 \\ 0, & n \text{ even} \\ -\frac{1}{n^2\pi^2\tau^2}, & n \text{ odd} \end{cases} \quad (12)$$

and the *Shepp-Logan* filter [7]

$$h(n\tau) = \begin{cases} \frac{2}{\pi^2\tau^2}, & n = 0 \\ -\frac{2}{n^2\pi^2(4\nu^2-1)}, & n \neq 0 \end{cases} \quad (13)$$

RESULTS

Two spectral lines were used for determining the population of argon excited states at 706 nm and 714 nm. The two lines correspond to the Ar I $[3s^23p^5(^2P_{1/2}^0)4p \rightarrow 3s^23p^5(^2P_{3/2}^0)4s]$ transition, for $J_i - J_k$ (2-2) and (2-1), respectively. We used smooth cubic spline approximation to smooth the noise in the measured signal of the plasmoid projections for the experimental data. The reconstructed populations of excited argon atoms are plotted in Figs. 4 and 5.

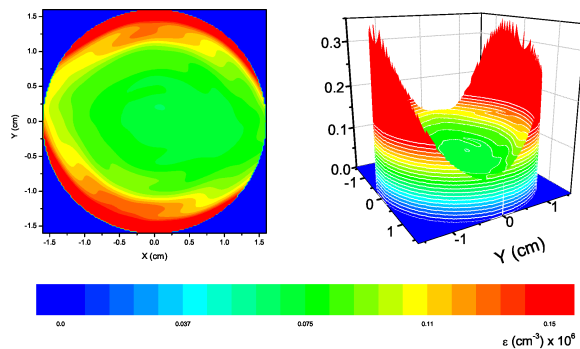


Figure 4: Population of the Ar I at 706.72 nm, 2.4 Torr, FBP with Ram-Lak filter.

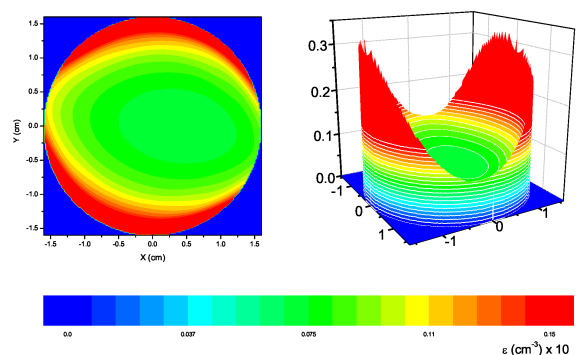


Figure 5: Population of the Ar I at 706.72 nm, 2.4 Torr, FBP with Shepp-Logan filter.

It is evident from the Figs. 4 and 5 that the excited Ar atoms are mainly concentrated close to the inner surface of

the quartz tube. This leads us to the conclusion that the discharge is partially sustained with a surface wave. Some parts in the population distribution are missing, which is due to our ability to measure a limited range of angles (48° - 168°). We obtained completely different results, in the case where no filters were used.

Our next step is to develop a wavelet based tomography model to be applied in beam dynamics physics. This model, unlike the Fourier transform, is localized spatially and can be applied even when a limited number of angular projections are available [8].

CONCLUSION

We have developed a tomography reconstruction model to study the collective effects in plasma. Our aim was to observe plasma internal dynamics using the measured emitted spectral line intensities of integrated data. Two filtered back projection approaches, Ram-Lak and Shepp-Logan, were employed. The model has been tested on supersonic flowing MW discharge maintained in a cylindrical quartz tube. The promising results allow us to introduce the tomography to obtain population distributions of excited neutral Ar species inside the single cell SRF niobium cavity.

REFERENCES

- [1] M. Rasković, J. Upadhyay, L. Vušković, M. S. Popović, A. M. Valente-Feliciano, and L. Phillips, Phys. Rev. ST. Accel. Beams. 13 (2010) 112001.
- [2] J. Radon, Math. -Phys. Kl. 69 (1917) 262.
- [3] V. Pickalov and T. Melnikova, Plasma tomography (in Russian) (Nauka, Novosibirsk, 1995).
- [4] G. E. Shilov, Mathematical analysis (in Russian) (Nauka, Moscow, 1965).
- [5] M. J. Lighthill, Introduction to Fourier Analysis and Generalised Functions (Cambridge University Press, Cambridge, Great Britain, 1959).
- [6] A. Rosenfeld and A. C. Kak, Digital picture processing (Academic Press, Inc., New York, New York, 1982).
- [7] L. A. Shepp and B. F. Logan, IEEE. Trans. Nucl. Sci. NS-21 (1974) 21.
- [8] C. Berenstein and D. Walnut, 75 Years of Radon Transform, Local inversion of the Radon transform in even dimensions using wavelets (International Press, Cambridge, Massachusetts, 1994).